Genetics and Molecular Research

# Metabolic response of LLC xenografted mice to oxythiamine, as measured by [$^1$H] NMR spectroscopy

**H. Lu[1], W.X. Lan[2], L. Bo[1], C. Niu[2], J.J. Zhou[1] and H.L. Zhu[1]**

[1]Department of Respiratory Medicine, Huadong Hospital, Fudan University, Shanghai, China
[2]Shanghai Institute of Organic Chemistry, Chinese Academy of Sciences, Shanghai, China

Corresponding author: H.L. Zhu
E-mail: zhuhuili999@126.com

Genet. Mol. Res. 14 (3): 11043-11051 (2015)
Received February 4, 2015
Accepted June 8, 2015
Published September 21, 2015
DOI http://dx.doi.org/10.4238/2015.September.21.17

**ABSTRACT.** Oxythiamine (OT) has been proven to be a potential anticancer drug. With the help of NMR-based metabonomics, we studied the metabolic changes within tumor-bearing mice with different levels of OT administration using a C57BL/6 mouse Lewis lung carcinoma tumor transplantation model. We administered different concentrations of OT (75, 150, 300, and 600 mg·kg$^{-1}$·day$^{-1}$) to the mice orally for 2 weeks, recorded animal weights and tumor volumes, sacrificed the animals, and collected blood and tumor mass samples for nuclear magnetic resonance determination. Compared with the findings for the control (untreated) group, the tumor weights and volumes of the 150, 300, and 600 mg·kg$^{-1}$·day$^{-1}$ groups decreased with no difference among these OT groups. A large metabolite difference was observed in plasma metabolites between the blank and control groups, which indicated the success of the tumor-bearing model. The metabolites in tumor associated with thiamine-dependent enzymes (TDEs) underwent considerable change between the OT and control groups, exhibiting concentration dependence and enzyme specificity. The restriction

 

of TDEs by OT may be a major mechanism underlying its anticancer effect. The role of OT as a potential anticancer drug and a dehydrogenase inhibitor should therefore be taken into consideration in future tumor research.

**Key words:** Oxythiamine; Thiamine-dependent enzymes; Tumor; Nuclear magnetic resonance; Metabonomics

## INTRODUCTION

In recent decades, researchers have found that oxythiamine (OT) exerts an inhibitory effect on tumor proliferation. OT can cause G1 cell cycle arrest in Ehrlich's ascites tumor cells (Rais et al., 1999) and its inhibition effects are associated with the deactivation of mitogen-activated protein kinase (MAPK) pathways in MIA PaCa-2 cells (Zhang et al., 2010). Transketolase activity and tumor cell proliferation decreased significantly after 200 $mg \cdot kg^{-1} \cdot d^{-1}$ OT treatment *in vitro* (Comin-Anduix et al., 2001). OT supplementation has been shown to attenuate tumor cell metastasis and apoptosis, possibly via multiple cellular signaling pathways (Yang et al., 2010; Wang et al., 2013). Although these results affirm the anticancer effects of this antivitamin derivative of thiamine, there is little data about the metabolite changes within tumors treated with OT. In this study, we have attempted to identify such changes using the platform of 1D $^1H$ nuclear magnetic resonance (1D [$^1H$] NMR) spectroscopy.

Metabonomics is a systemic approach for studying *in vivo* metabolic profiles that promises to provide information on drug toxicity, disease processes, and gene function at several stages in the discovery and development process (Nicholson et al., 1999, 2002). Principal component analysis (PCA), partial least squares-discriminant analysis (PLS-DA), and orthogonal signal correction PLS-DA (OSC-PLS-DA) were applied to analyze NMR spectroscopy data (Trygg et al., 2007). In order to track the metabolism changes clearly, four treatment groups were established, incorporating low, middle, high, and super high dose administration of 75, 150, 300, and 600 $mg \cdot kg^{-1} \cdot d^{-1}$ OT, respectively.

## MATERIAL AND METHODS

### Reagents and equipment

Reagents and equipment were obtained from the following suppliers as indicated: OT (Sigma-Aldrich, St. Louis, MO, USA); 70% perchloric acid ($HClO_4$), potassium hydrate (KOH) (Mu Yuan Biological Science and Technology Co. Ltd., Shanghai, China); 3-(trimethylsilyl) propionic-2,2,3,3-$d_4$ acid, sodium salt (TSP) (Merck KGaA, Darmstadt, Germany); 99.9% deuterated water ($D_2O$) (Sigma); phosphate buffered saline (PBS) ($K_2HPO_4/NaH_2PO_4$, 150 mM, pH 7.4); 5810R ultracentrifuge (Eppendorf, Hamburg, Germany); Varian INOVA-600 NMR 599.9 MHz spectrometer (Varian Inc., Palo Alto, CA, USA); and a freeze dryer (Martin Christ, Osterode, Germany).

### Cell culture

The mouse Lewis lung carcinoma (LLC) cell line was purchased from the Shanghai Institutes for Biological Sciences (SIBSCAS). LLC cells were cultured in Dulbecco's modified Eagle medium (DMEM) (Ginuo Biological Medicine Technology Co. Ltd., China) containing

 

10% (v/v) fetal bovine serum (FBS) (Gibco, Gaithersburg, MD, USA) and penicillin (100 kU/L) and streptomycin (100 kU/L) in a humidified incubator (Thermo Fisher Scientific, Waltham, MA, USA) under 5% $CO_2$ and 95% air at 37°C. The cells were maintained as monolayers in culture flasks using 0.05% trypsin (Gibco) and counted.

## Animal models

Specific pathogen-free C57BL/65 male mice (N = 60, 18-22 g) were purchased from the Animal Experimental Center of the Pharmacy College of Fudan University. During the accommodation and experimental periods, animals were provided free access to standard rodent feed (Shilin Biological Technology Co. Ltd., Shanghai, China) and water. The standard diet contained 22.6% crude protein, 4.9% crude fat, and 3.3% crude fiber as indicated by the supplier. A blank group (group A) was established consisting of ten mice, and the remaining fifty animals were implanted subcutaneously in the right forelimb axillary with 2 x $10^7$ LLCs/mouse (0.1 mL). These fifty mice were randomly divided into five groups of ten animals each: the control (group B, untreated), and treatment groups C-F which received 75, 150, 300, or 600 $mg \cdot kg^{-1} \cdot day^{-1}$ OT, respectively. The corresponding amounts of OT (dissolved in 0.2 mL normal saline) were administered daily beginning on the day after implantation; the A and B groups were given equivalent amounts of normal saline. Animals were weighed every other day and the lengths and widths of the xenografted tumors were measured every other day from the 5th day after implantation (tumor volume = length x $width^2/2$). At the 15th day, all mice were sacrificed and plasma and tumor tissues were collected for NMR testing.

## Sample preparation

A 200-µL plasma aliquot was mixed with 90 µL PBS and 230 µL $D_2O$, centrifuged at 12,000 *g* for 10 min at 4°C, and transferred to 5 mm NMR tubes. Frozen tumor tissues were weighed, powdered in the presence of liquid nitrogen, homogenized in 2 mL ice-cold 10% perchloric acid, vortexed for 30 s, and centrifuged again at 12,000 *g* for 10 min at 4°C. The supernatant was neutralized with 1.0 M KOH to a pH of 7.2, and the extracts were centrifuged again as previously. The final supernatant (water-soluble phase) was lyophilized overnight at -45°C in the freeze dryer. The lyophilized sample was redissolved with 530 µL PBS and 10 µL TSP (1 mg/mL), centrifuged as previously, and transferred to 5 mm NMR tubes.

## [$^1$H]-NMR spectra detection and processing

Samples were analyzed by [$^1$H] NMR spectroscopy using a 599.9 MHz Varian INOVA-600 spectrometer at 298 K. All NMR spectra were phased and baseline corrected using the MestReNova 8.1.4 software (Umetrics, Umeå, Sweden); plasma spectra were referenced to the lactate methyl signal at δ1.33 and tissue spectra were referenced to the TSP signal at δ0.0. Plasma spectra were reduced to segments of 0.01 ppm between 0.8 and 4.6 ppm and tissue spectra were reduced to segments of 0.01 ppm between 0.5 and 9.5 ppm. The water region from 4.60 to 5.20 ppm was subsequently excluded. Each spectral intensity data set was normalized to the total sum of the spectral regions. The resulting data sets were then converted to the Microsoft Office Excel 2007 (Microsoft Inc., Redmond, WA, USA) format and imported into SIMCA-P 13.0 (Umetrics, Umeå, Sweden) for multivariate analysis.

## Data analyses

PCA results were presented using a "scores plot" with a series of principal components carrying all the information of the data and loading plots. A dot in the scores plot represented a sample and the clustering tendency of these dots suggested the metabolic characteristics of each group in the model. PLS-DA and OPLS-DA were applied to further analyze the metabolic changes for strengthening differences among groups and reducing negative effects of correlative factors but required validation testing. Cross-validation (CV), permutation tests, and CV-ANOVA are the most common validation testing methods for PLS-DA and OPLS-DA and were carried out using the SIMCA-P 13.0. After validation, we selected metabolites with significant differences among the passed groups model established by Pearson's correlation coefficients analysis in OPLS-DA using correlation coefficient loading plots.

# RESULTS

## Growth conditions of xenografted tumors

We found no differences in tumor formation time among tumor-bearing mice. From the 5th day, nodules could be touched or seen and those in the B group enlarged fastest. The tumor weights of the D (3.05 ± 0.74 g), E (2.74 ± 0.63 g), and F (2.54 ± 0.50 g) groups diminished significantly compared with those of the B group (4.24 ± 0.80 g); the tumor volumes of the D (1815.35 ± 422.82 $mm^3$), E (1667.39 ± 396.02 $mm^3$), and F (1599.10 ± 321.28 $mm^3$) groups were also obviously smaller than those of the B group (2562.33 ± 641.25 $mm^3$). There was no difference in tumor weights or volumes among the OT groups.

## $^1$H-NMR spectra determination

### *Metabolic profiling of samples*

The major and significant metabolites in the spectra were identified according to data presented in the literature (Nicholson et al., 1995; Lindon et al., 1999) and in the public shared metabolite database HMDB (http://www.hmdb.ca/) as well as from the characteristics of the chemical shifts and peak splitting modes (Figure 1).

### *$^1$H-NMR spectra pattern recognition with PCA, PLS-DA, and OPLS-DA*

PCA included all the groups and the distribution of metabolic trend and outliers can be judged directly (Figure 2A and B). In PLS-DA and OPLS-DA, we validated the reliability of the matching models with the appropriate methods (cross-validation, permutation tests, and CV-ANOVA). Results from these analyses showed that, from the plasma models (Figure 2C), blank group (A) with control group (B) and control group (B) with OT group (F) passed validation (model parameters respectively, $R^2X = 0.442$, $R^2Y = 0.893$, $Q^2 = 0.61$, and $P = 0.0012$; $R^2X = 0.508$, $R^2Y = 0.938$, $Q^2 = 0.871$, and $P = 0.0003$; where $Q^2 > 0.4$ and $P < 0.05$ is the standard for model validation). In the tumor tissue models (Figure 2D), the comparisons of the control group (B) with OT groups (C-F) all passed validation (model parameters respectively,

$R^2X = 0.523$, $R^2Y = 0.806$, $Q^2 = 0.615$, and $P = 0.0038$; $R^2X = 0.497$, $R^2Y = 0.893$, $Q^2 = 0.732$, and $P = 0.0008$; $R^2X = 0.589$, $R^2Y = 0.897$, $Q^2 = 0.819$, and $P < 0.0001$; $R^2X = 0.478$, $R^2Y = 0.938$, $Q^2 = 0.871$, and $P < 0.0001$). The $Q^2$ and P values of the tumor models increased gradually indirectly indicating that metabolic changes increased with increase in the dose of OT administered, within the respective tumor tissue. The larger of $Q^2$ and the smaller of P values indicate the bigger difference of metabolic changes between the two groups in the model.

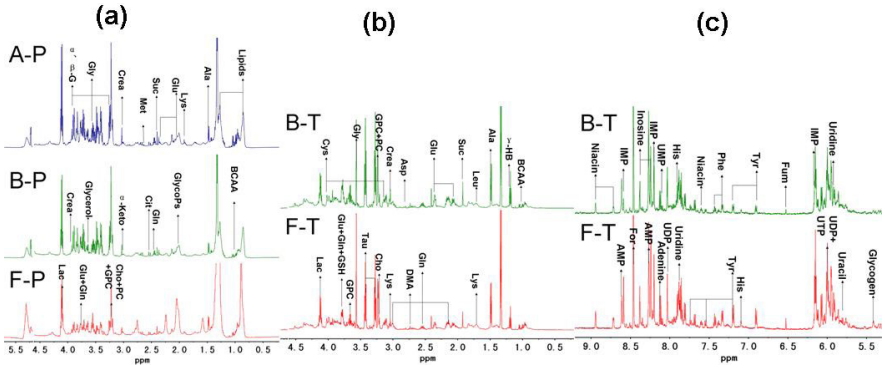


**Figure 1.** Representative $^1$H-NMR spectra of plasma and tumors acquired at Varian INOVA-600 spectrometer of 599.9 MHz. **a.** Plasma $^1$H-NMR spectra at 0.5-5.5 ppm of A, B, and F groups. **b.** Tumor tissue $^1$H-NMR spectra at 0.5-4.5 ppm of B and F groups. **c.** Tumor tissue $^1$H-NMR spectra at 5.5-9.0 ppm of B and F groups. Keys: BCAA, branched chain amino acids; $\gamma$-HB: $\gamma$-hydroxybutyric acid; Lac, Lactate; Ala, Alanine; Lys, Lysine; Cys, Cysteine; Glu, Glutamate; Gln, Glutamine; GSH/GSSG, glutathione; GlycoPs, Glycoproteins; Pyr, Pyruvate; Suc, Succinate; Cit, Citrate; Met, Methionine; DMA, Dimethylamine; TMAO, Trimethylamino oxide; $\alpha$-Keto, $\alpha$-Ketoglutarate; Crea, Creatine; Phe, Phenylalanine; Try, Tryosine; His, Histine; Cho, Choline; PC, phosphorylcholine; GPC, Glycerophosphocholine; Tau, Taurine; $\alpha$ or $\beta$-G, Glucose; Gly, Glycine; Fum, Fumarate; For, Formate.

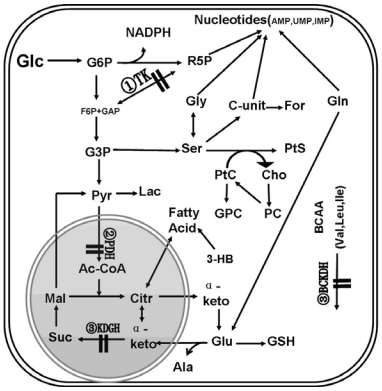


**Figure 2.** Metabolic pathways with relevant metabolites involved in our model. Only metabolic pathways with the most convincing evidences of involvement in transplanted tumors are represented. TK is the first enzyme inhibited (①); PDH is the second enzyme inhibited (②); KGDH and BCKDH follow up (③). ‖ indicates an inhibition sign. The grey area represents the mitochondria metabolism. Keys: Glc, Glucose; G6P, 6-P-Glucose; F6P+GAP, 6-P-Fructose+3-P-Glyceraldehyde; R5P, 5-P-Ribose; NADPH, nicotinamide-adenine dinucleotide phosphate; G3P, 3-P-Glycerate; Ac-CoA, acetyl-CoA; Citr, Citrate; Mal, Malate; Ser, Serine; C-unit, one-carbon unit; PtS, phosphatidylserine; BCAA, branched chain amino acid; Val, Valine; Leu, Leucine; Ile, Isoleucine; thiamine dependent enzymes (TDEs): TK, transketolase; PDH, pyruvate dehydrogenase; KGDH, ketoglutarate dehydrogenase and BCKDH, branched-chain α-ketoacid dehydrogenase.

### *Changes of significant metabolites among tumor groups (B-F)*

Using correlation coefficient loading plots and $r_{cutoff}$ values, we determined the significant metabolites and have listed these along with their corresponding r values in the validated group models (Table 1). Figure 3 shows the metabolic pathways involved in the tumor response.

**Table 1.** Significant metabolites of $^1$H-NMR spectra with corresponding r among Plasma and Tumor Tissue models.

| Metabolites | Chemical Shift (ppm) | Plasma | | Tumor tissue | | | |
|---|---|---|---|---|---|---|---|
| | | AB r = 0.632 | BF r = 0.632 | BC r = 0.602 | BD r = 0.632 | BE r = 0.632 | BF r = 0.602 |
| AMP | **8.60s**, 8.27s, 6.15d, 4.03m, 4.38m, 4.52m | | | **-0.65** | **-0.68** | **-0.70** | **-0.75** |
| UMP | 5.98, 5.99m, **8.12d**, 4.25, 4.34, 4.41m, 3.97 | | | **-0.61** | **-0.78** | **-0.76** | **-0.80** |
| NADPH | 6.04d, 6.09d, **8.14s**, 8.18dd, **8.42s**, 8.82d | | | **0.69** | **0.71** | 0.39 | -0.28 |
| Glycine | 3.57s | **-0.74** | 0.33 | **0.63** | **0.67** | **0.66** | **0.87** |
| Formate | 8.46s | | | **0.75** | **0.78** | **0.80** | 0.50 |
| γ-HB | **1.20d**, 2.31dd, 2.38dd, 4.23m | | | **0.61** | **0.71** | **0.86** | 0.55 |
| Glycerol | **3.56dd, 3.65m**, 3.79m | -0.55 | **-0.72** | **0.65** | **0.66** | **0.87** | **0.76** |
| Citrate | 2.55d, 2.68d | 0.1 | **-0.76** | -0.42 | **-0.74** | -0.54 | -0.39 |
| Glutamate | 2.06m, 2.13m, **2.36m**, 3.77t | **-0.75** | -0.40 | -0.57 | **-0.63** | **-0.83** | **-0.93** |
| Glutamine | 2.15m, 2.46q, **3.78m** | **-0.83** | **-0.75** | -0.47 | **-0.67** | **-0.69** | -0.54 |
| GSH/GSSG | **2.15m**, 2.54q, 3.79m——Glu<br>2.97m, 3.32m, 4.77m——Cys | **-0.73** | -0.46 | -0.55 | **-0.70** | **-0.93** | **-0.96** |
| Glycerophosphocholine (GPC) | **3.23s**, 3.68t, 4.32t | | | -0.54 | **-0.77** | **-0.88** | **-0.87** |
| Myoinositol | 3.28t, 3.56dd, **3.63dd**, 4.06t | **-0.92** | **-0.82** | -0.1 | **-0.7** | **-0.87** | **-0.80** |
| β-Glucose | 3.26dd, **3.42dd**, **3.47dd**, 3.50dd, 3.90dd, 4.65d | -0.45 | **-0.87** | 0.56 | **0.63** | **0.70** | 0.27 |
| α-Glucose | **3.41t**, 3.53dd, 3.71t, 3.74m, 3.84m, 5.23d | | | | | | |
| Lactate | **1.33d**, 4.11q | -0.55 | 0.27 | 0.39 | **0.63** | 0.29 | 0.22 |
| Leucine | **0.96d, 0.97d**, 1.71m, 3.73t | **-0.68** | 0.61 | -0.29 | **0.67** | **0.70** | **0.60** |
| Succinate | 2.41s | -0.61 | 0.43 | 0.12 | -0.1 | **-0.63** | **-0.76** |
| IMP | 8.20s, 8.57s, **6.16d**, 4.02d, 4.26d, 4.52d, 4.78d | | | -0.35 | -0.55 | **-0.74** | **-0.87** |
| Isoleucine | **0.94t, 1.01d**, 1.26m, 1.48m, 1.98m, 3.68d | **-0.83** | **-0.79** | -0.23 | 0.42 | **0.64** | 0.46 |
| Valine | **0.99d, 1.04d**, 2.28m, 3.62m | **-0.85** | 0.41 | -0.39 | 0.50 | **0.63** | 0.45 |
| Alaine | **1.48d**, 3.78q | -0.40 | 0.50 | 0.27 | 0.57 | **0.67** | **0.71** |
| Phosphocholine (PC) | **3.23s**, 3.61t, 4.21t | -0.43 | **-0.76** | 0.25 | 0.50 | **0.65** | 0.48 |
| Creatine | **3.04s**, 3.94s | **-0.79** | 0.10 | 0.20 | -0.40 | -0.39 | **-0.73** |
| Taurine | 3.27t, 3.43t | | | 0.5 | 0.1 | -0.3 | **-0.79** |
| Choline | **3.21s**, 3.51t, 4.07t | **-0.66** | -0.55 | 0.32 | 0.47 | 0.59 | -0.56 |

r is a correlation coefficient between metabolites and model whose absolute value has a positive correlation with the contribution of corresponding metabolites for separating two groups. Each metabolite has its r value in a model, only when $|r| \geqslant r_{cutoff}$, the change of the metabolite is significant. Here $r_{cutoff}$ is fixed at 0.602 (N = 10) and 0.632 (N = 9) ("n" refers to sample number of the less group). Bold r value is considered significant. Negative r means that the later group is less than the former and vice versa. For example, AMP, r = -0.65 in the tumor tissue BC group model ($r_{cutoff}$ = 0.602), means the AMP of C group is less than B group. Bold chemical shifts are the spectra peaks used for analysis. Peak multiplicity: s = singlet; d = doublet; t = triplet; q = quartet; dd = doublet of doublets; m = multiplet.

In the plasma models, many metabolites, including branched chain amino acid (BCAA), glutamate, glutamine, GSH, succinate, creatine, choline, myoinositol, and glycine, declined markedly in the B group compared with the A group, which indicates that we successfully duplicated a tumor cachexia model. We found no changes among the plasma metabolites in the B-E groups; however obvious differences were found between the B and F groups in glucose, citrate, glutamine, myoinositol, and phosphocholine levels, which decreased markedly.

 

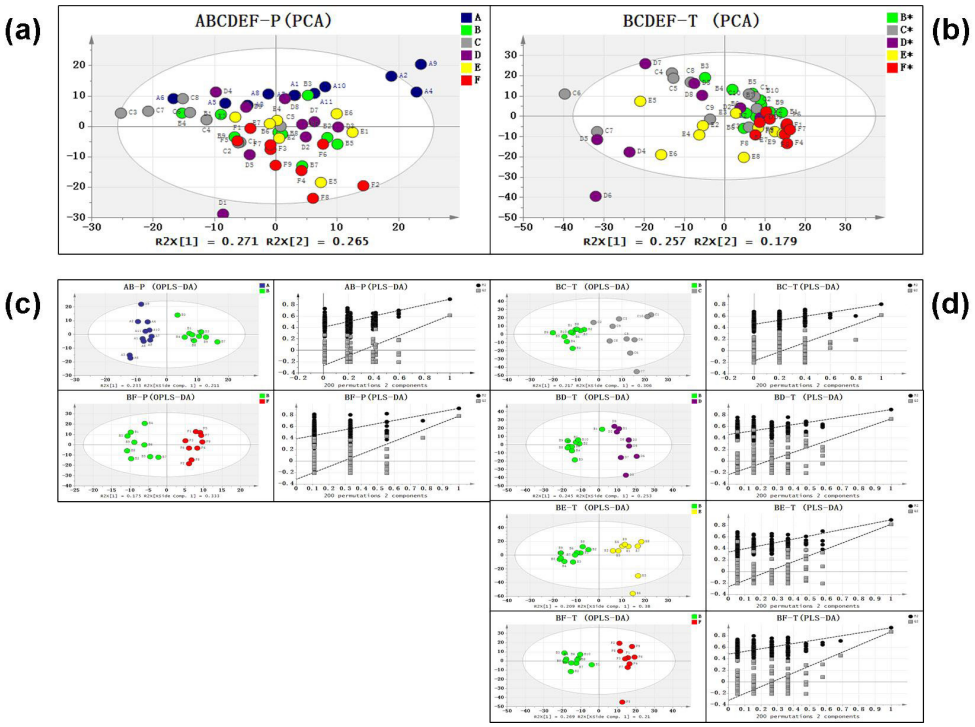


**Figure 3.** Plasma and tumor tissue PCA Scores Plot of all groups and OPLS-DA Scores Plots with corresponding permutation tests in PLS-DA of the models passing validation. These plots are acquired from SIMCA-P 13.0. **a. b.** The distribution of metabolic trend and outliers can be judged in PCA Scores Plot. We select first two principal components carrying the major information of the whole data. $R^2X[1] = 0.271$ means the first principal component carry 27.1% of the total information and $R^2X[2] = 0.265$ means the second principal component carry 26.5%. **c. d.** In OPLS-DA Scores Plots, passed models show a satisfactory separation effect with two principal components ($N_{pc} = 2$); In Permutation Tests, black dots and dash line refers to $R^2$ and the grey refers to $Q^2$, the closer of $R^2$ and $Q^2$, the closer to 1, the greater of the line slope, will make the model more reliable; P, plasma. T, tumor tissue.

In C group tumor tissue in which transketolase (TK), an enzyme extremely dependent upon thiamine, had been inhibited, the levels of AMP and UMP noticeably decreased whereas NADPH, glycerol, glycine, formate, and γ-HB increased. Reduction in ribose-5-phosphate resulted from the inhibition of the nonoxidative branch of Pentose Phosphate Pathway (PPP) regulated by TK. Simultaneously, other precursors of *de novo* nucleotide biosynthesis such as glycine and C-unit (the major product of which is formate) were driven to accumulate. The observed increase in NADPH might also be related to the enhancement of the of the oxidative branch of PPP to make up the shortage of ribose, although the sources of NADPH in tumor cells are complex.

In D group tumor tissue, the levels of citrate, glutamate, glutamine, GSSG, GPC, and myoinositol began to decrease, whereas those of glucose, lactate, and leucine increased. Thiamine is also a coenzyme for two other dehydrogenases, pyruvate dehydrogenase (PDH), and α-ketoglutarate dehydrogenase (KGDH). The inhibition of PDH can result in cleavage of the acetyl-CoA from pyruvate for use in citrate synthesis. From the anaplerotic metabolism

of glutamine/glutamate, tumor cells acquire adequate α-ketoglutaric acid to maintain the Kreb's cycle. Pyruvate, the upstream precursor of PDH, is driven to conversion into lactate to avoid excess accumulation, which in turn becomes elevated slightly; the net effect is that the availability of glucose declines as a result of the inhibition of the TK and PDH mediated metabolic pathways. As the level of OT increased and its effects became elevated, the activity of branched-chain alpha-keto acid dehydrogenase (BCKDH), another thiamine dependent enzyme, was reduced, resulting in the selective accumulation of BCAA, leading to an increase in leucine.

In E group tumor tissue, the levels of succinate declined sharply due to the inhibitory effect of OT on KGDH and the strong restriction of tricarboxylic acid (TCA). Alanine, a major product of glutaminolysis, increased; two other BCAAs, valine and isoleucine, accumulated as had leucine. These results presented above show that dosages of up to 300 $mg \cdot kg^{-1} \cdot d^{-1}$ OT resulted in the limitation of TK, PDH, KGDH, and BCKDH to varying degrees.

## DISCUSSION

OT is phosphorylated in the same manner as is thiamine by the enzyme thiamine pyrophosphokinase to create thiamine pyrophosphate (TPP), a cofactor for several enzymes, including TK, in the non-oxidative pathway; PDH and KGDH in glucose metabolism; and other enzymes such as BCKDH in amino acid metabolism, which are called thiamine dependent enzymes (TDEs). Thus, as TPP is required by enzymes that catalyze important reactions, OT is therefore expected to exhibit cell-type-specific confounding pleiotropic effects. From the results presented above, TK was found to be limited following administration of 75 mg/kg OT, PDH was restricted by 150 mg/kg OT, and KGDH and BCKDH levels were limited in mice subjected to 300 mg/kg OT.

The importance status of TK in tumorigenesis is uncontested as it can provide adequate ribose molecules for rapid proliferation. TK has been shown to be a sensitive TDE which is a main reason underlying the anticancer effect of OT. In this study, TK activity and tumor cell proliferation decreased significantly after eight days of treatment with 200 $mg \cdot kg^{-1} \cdot d^{-1}$ OT in an Ehrlich's ascites tumor cell transplanted mouse model (Thomas et al., 2008). Comparatively, a preferential reduction of TK activity was observed in tumors over that of another TDE, KGDH in HCT-116 tumor-bearing nude mice which had received 100 mg/kg OT intravenously on alternate days for two weeks (Comin-Anduix et al., 2001). In our results, we found that TK was reduced following administration of 75 mg/kg OT without effect on tumor size.

PDH, another TDE, has been generally ignored in research programs and especially in tumor research. It is well known that PDH is inactivated through phosphorylation by overexpression of pyruvate dehydrogenase kinases in malignant tissues. However, the significant decrease of citrate observed following 150 mg/kg OT treatment supports the existence and function of PDH in tumor models, which should be explored further. Research has shown that PDH might translocate from the mitochondria to the nucleus suggesting a potential role in disease states associated with proliferative signals or mitochondrial dysfunction, such as cancer (Sutendra et al., 2014).

KGDH is a less sensitive TDE compared to TK and PDH. Oxidation of α-ketoglutarate is required for reductive carboxylation with the catalysis of KGDH in cancer cells with mitochondrial defects. Silencing KGDH can alter the cellular redox state and substantially suppress reductive carboxylation (Mullen et al., 2014). The decreasing of BCAAs following

OT treatment suggests that BCKDH has also been restricted in this model. BCKDH catalyzes the irreversible oxidative decarboxylation of the three branched-chain α-ketoacids obtained by the deamination of the branched-chain amino acids. Immunoblot analyses indicate that BCKDH inhibition might be a mechanism of thiaminase-mediated toxicity.

In the 600 mg/Kg OT group, all TDEs should have been restricted which are the key enzymes of PPP and TCA cycle. Therefore, it is reasonable to speculate that 600 $mg \cdot kg^{-1} \cdot d^{-1}$ OT might be approaching a toxic dose. Overall, these results suggest that the changes in internal metabolites observed following different degrees of OT exposure reflect the differential restriction of TDEs, which is primarily responsible for the anticancer effects of OT. OT is consequently not only a potential anticancer drug but also a dehydrogenase inhibitor, which should be taken into consideration in future tumor research.

## Conflicts of interest

The authors declare no conflict of interest.

## ACKNOWLEDGMENTS

Research supported by a Grants-in-Aid of Basic Research Key Project from the Shanghai Science and Technology Commission (#12JC1402202). The authors thank the staff of the Experimental Animal Center, College of Pharmacy, Fudan University for their technical assistance with the animals, and the staff of the Shanghai Institute of Organic Chemistry, Chinese Academy of Sciences for their NMR technical assistance in these studies.

## REFERENCES

Comin-Anduix B, Boren J, Martinez S, Moro C, et al. (2001). The effect of thiamine supplementation on tumour proliferation. A metabolic control analysis study. *Eur. J. Biochem.* 268: 4177-4182.

Lindon JC, Nicholson JK and Everett JR (1999). NMR spectroscopy of biofluids. *Annu. Rep. NMR Spectroscopy* 38: 1-88.

Mullen AR, Hu Z, Shi X, Jiang L, et al. (2014). Oxidation of alpha-ketoglutarate is required for reductive carboxylation in cancer cells with mitochondrial defects. *Cell Rep.* 7: 1679-1690.

Nicholson JK, Foxall PJ, Spraul M, Farrant RD, et al. (1995). 750 MHz 1H and 1H-13C NMR-spectroscopy of human blood-plasma. *Anal. Chem.* 67: 793-811.

Nicholson JK, Lindon JC and Holmes E (1999). 'Metabonomics': understanding the metabolic responses of living systems to pathophysiological stimuli via multivariate statistical analysis of biological NMR spectroscopic data. *Xenobiotica* 29: 1181-1189.

Nicholson JK, Connelly J, Lindon JC and Holmes E (2002). Metabonomics: a platform for studying drug toxicity and gene function. *Nat. Rev. Drug Discov*. 1: 153-161.

Rais B, Comin B, Puigjaner J, Brandes JL, et al. (1999). Oxythiamine and dehydroepiandrosterone induce a G1 phase cycle arrest in Ehrlich's tumor cells through inhibition of the pentose cycle. *FEBS Lett.* 456: 113-118.

Sutendra G, Kinnaird A, Dromparis P, Paulin R, et al. (2014). A nuclear pyruvate dehydrogenase complex is important for the generation of acetyl-coA and histone acetylation. *Cell* 158: 84-97.

Thomas AA, Le Huerou Y, De Meese J, Gunawardana I, et al. (2008). Synthesis, *in vitro* and *in vivo* activity of thiamine antagonist transketolase inhibitors. *Bioorg. Medic. Chem. Lett.* 18: 2206-2210.

Trygg J, Holmes E and Lundstedt T (2007). Chemometrics in metabonomics. *J. Proteome Res*. 6: 469-479.

Wang J, Zhang X, Ma D, Lee WN, et al. (2013). Inhibition of transketolase by oxythiamine altered dynamics of protein signals in pancreatic cancer cells. *Exp. Hematol. Oncol.* 2: 18.

Yang CM, Liu YZ, Liao JW and Hu ML (2010). The *in vitro* and *in vivo* anti-metastatic efficacy of oxythiamine and the possible mechanisms of action. *Clin. Exp. Metastasis* 27: 341-349.

Zhang H, Cao R, Lee WP, Deng C, et al. (2010). Inhibition of protein phosphorylation in MIA pancreatic cancer cells: confluence of metabolic and signaling pathways. *J. Proteome Res.* 9: 980-989.